Performance Analysis and Modelling of a Radio Frequency Energy Harvesting System

Cosmin CIRSTEA, Teodor PETRITA, Viorel POPESCU, Aurel GONTEAN
Politehnica University of Timisoara, 300223, Romania
cosmin.cirstea@etc.upt.ro

***Abstract*—The development of autonomous battery powered systems which can be deployed in inaccessible locations for sensing applications has determined the development of various energy harvesting systems. Such an energy harvester is the one developed by Powercast which can convert the energy of radio frequency signals into useful power. A model of the harvested power can prove to be a useful tool for simulation purposes as it can provide, to some extent, prior knowledge of available energy resources when optimally deploying sensor networks.**

To obtain an accurate model of the harvested energy we have developed an experimental setup which has been used to determine the harvested power in two different environments, a hallway and a parking lot. We have developed the experimental setup to determine the amount of power available at the output of the radio frequency harvester which consists of a current measurement system and a data acquisition system. We have also modeled through simulations the harvested power based on the characteristics of the transmitter and receiver antennas and those of the environment.

We have compared the results obtained through in field measurement with the ones obtained through simulation and we have shown that within certain margins of error of maximum 2 dBm one can successfully predict the amount of energy the system can harvest. However the RF-DC and Boost converter efficiency are also key factors in the quantity of harvested energy.

***Index Terms*—energy harvesting, experimental setup, modelling, performance analysis, radio frequency, simulation.**

I. Introduction

Wireless sensor networks (WSNs) represent a specific type of networks due to their unique characteristics such as low cost, small dimensions, limited power resources and self-organization capabilities. Such networks are used in a variety of applications that range from environmental to healthcare monitoring, industrial automation and even military surveillance [1-2] to mention just a few. On one hand WSNs provide endless opportunities for monitoring and data gathering but at the same time pose serious challenges when considering the fact that energy is scarce and thus network lifetime is limited. As most applications that use WSNs require in field deployment where human access is seldom possible, efficient energy consumption combined with any form of energy harvesting, such as solar [3], thermal or mechanical [4], provide very attractive solutions for extending the lifetime of such networks.

Efficient energy consumption can be obtained at the node level by using intelligent sleep/wake up intervals [5] and also at the network level through adequate routing algorithms combined with data aggregation and fusion techniques [6-7].

Radio frequency energy harvesting is the process through which ambient energy from various radio transmitters is captured by a receiving antenna and converted into useful power. The same principle is used in passive radio frequency (RF) identification (RFID) devices which are powered when subject to a signal of a certain frequency and power. Usually, in order to obtain useful power levels from radio frequency the receiver must be either in close proximity to the transmitter or must be subject to many transmitting signals.

In a recent study by Le et al. [8], a RF-DC power conversion system is described which can efficiently convert far-field RF energy to DC voltages for low received power. The presented system can operate at a distance of maximum 44 meters with a received signal power as low as 5.5 μW (-22.6 dBm) from a 4W Effective Isotropic Radiated Power (EIRP) radiation source. According to the authors [8] the system can provide a voltage of 1V DC and 0.3 μA at a distance of 15 meters. Other examples of energy harvesting systems are the ones developed by Powercast which are 915 MHz based devices that convert RF energy received from a transmitter into effective DC power using the P2110 [9] RF-DC converter. The energy harvested can be used to power a sensor node or to recharge a battery. Such a device represents the basis for our experiments and a detailed description is available in section II.

The rest of this paper is organized as follows: section II describes the radio frequency energy harvesting system that has been analyzed and modeled, section III presents the model used for predicting the input power, section IV shows how the measurement of available charge has been performed, in section V the results obtained through experiments are described and section VI concludes this paper and presents future work.

II. Description of the Energy Harvesting System

In order to determine the performance of an RF energy harvester and find out the amount of energy which can be harvested and what it can be used for we have evaluated the Powercast P2110-EVAL-01 Energy Harvesting Kit for Wireless Sensors [10]. The kit consists of the following:

- One TX91501, a 3W EIRP 915 MHz transmitter with an 8.1 dBi gain integrated antenna [11].
- Two dipole (omnidirectional, 1.0 dBi gain) and two patch (directional 6.41 dBi gain) antennas.

This work was partially supported by the strategic grant POSDRU 88/1.5/S/50783, Project ID 50783 (2009), co-financed by the European Social Fund – Investing in People, within the Sectorial Operational Programme Human Resources Development 2007-2013.

Digital Object Identifier 10.4316/AECE.2013.01005

- Two P2110 energy harvesting boards which convert the received signal from the TX91501 transmitter with the help of the P2110 RF integrated circuit (IC) and store it in a capacitor.
- Two wireless sensor boards that can be attached to the P2110 PCBs which when powered, provide temperature, humidity and light information through a 2.4 GHz radio module.
- One access point development platform, which receives data packets from the two previously mentioned 2.4 GHz wireless sensor nodes, and interfaces with a PC for data output.

The key feature of this energy harvesting kit is the P2110 915MHz Powerharvester IC [9] which converts the received RF signal to DC and stores it in a capacitor, as can be seen in Fig. 1.

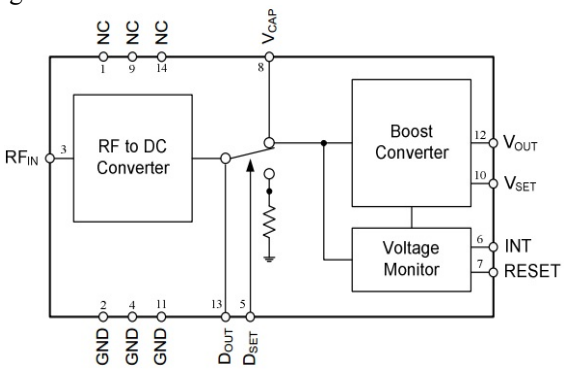

Figure 1. Block diagram of the P2110 Powerharvester Receiver IC [9]

When a voltage threshold is reached (1.8V) on the capacitor (VCAP output), enough energy has been harvested to either power the 2.4 GHz wireless sensor node for data acquisition and transmission or to enable the boost converter to provide a regulated voltage output of 3.3 V which can be boosted up to 5.25 V depending on the desired user application. The circuit is internally matched to 50 Ω, can operate down to -11.5 dBm input power and can provide a maximum output current of up to 50 mA [9].

III. Modelling Power Transfer

A. Far field range

Since experiments were performed with the Powercast module, we shall evaluate the far field range. As the transmitting antenna is a patch type antenna, with patch surface no more than 171.45 x 158.75mm, the casing size [11], the far field range (margins of the Fraunhoffer zone) for the antenna can be determined using the following formula [12]:

$$R_f > \frac{2 \cdot D^2}{\lambda}, \tag{1}$$

where D is „the largest dimension of the antenna" [13], in this case the diagonal of the antenna (233.65mm), and λ is the wavelength of the radio wave (327.64mm for 915MHz). The formula is used when $D > \lambda$ which is not the case here. Otherwise far field can be safely considered starting from 3 λ [14] which means that the far field range starts approximately 1m from antenna. Since we are interested in finding the coverage range of the power harvesting link, we will use the far field model.

B. Modelling antenna pattern

The transmitter module has the half power beam-width (HPBW) of 60° in both planes, with vertical polarization according to the producer. In standard right handed spherical coordinate system [15], with the antenna placed in origin point, the gain of the antenna can be calculated as follows:

$$G(\theta,\varphi) = G_0 \cdot \sin^{2p}\theta \cdot \cos^{2q}\frac{\varphi}{2} \tag{2}$$

where G_0 is the antenna gain (adimensional), θ is the declination, and φ is the azimuth. Exponents $p = 2.41$ and $q = 10$ are calculated from HPBW condition [16]. Antenna gain is stated in the datasheet as being $g_0 = 8.1\ dBi$ (logarithmic), but there is no indication of transmitter power, but rather of *EIRP* as being $P_{eir} = 3W$. The expected gain of such an antenna will be [16]:

$$g_0 = 45.1 - 10 \cdot \log_{10}(HPBW_{horiz} \cdot HPBW_{vert}) = 9.5\,dBi \tag{3}$$

where HPBWs in horizontal and vertical cuts are in degrees. The basis of this formula can be found in [17] and even if this is an approximative formula, we can take into account the lower value of manufacturer datasheet gain due to the dielectric (PCB) losses. This supposition is confirmed also by the reception antenna, also a dipole, with a gain of $g_d = 1\ dBi$, then non-logarithmic value for the dipole gain is $G_d = 1.26$. Thus, the power density pattern (excluding floor reflection) for the transmitter would be:

$$S(r,\theta,\varphi) = \frac{P_{eir}}{4\pi \cdot r^2} \cdot \sin^{4.82}\theta \cdot \cos^{20}\frac{\varphi}{2} \tag{4}$$

where r is the distance from the transmitting antenna. In fact, we have used so called "product formula" or "sum formula" for 3-D pattern interpolation [18]. Keeping in mind that the receiving dipole antenna is at the same height as the transmitting antenna ($\theta = \pi/2$) and oriented towards transmitter, the direct link budget would be, in *mW*:

$$P_{rx}(r,\theta,\varphi) = \frac{P_{eir}}{4\pi \cdot r^2} \cdot \sin^{4.82}\frac{\pi}{2} \cdot \cos^{20}\frac{\varphi}{2} \cdot \frac{\lambda^2}{4\pi} \cdot G_d \cong \frac{2.04}{r^2} \cdot \cos^{20}\frac{\varphi}{2} \cdot G_d \tag{5}$$

G_d was preserved separately in (5) – the since there are other versions of receiving/harvesting antennas with different gain. It is easy to spot out in (5) that at 1m from main radiation direction, harvested power should be about 2mW with 0 *dBi* antenna.

C. Modelling ground reflections

Since measurements were performed on a marble floor, we will determine the received power also considering the influence of ground reflection. Considering various sources we have chosen a value of electric permittivity between 8 and 10 in GHz range for marble and approximately 10 for dry asphalt. We have chosen according to [19-21] εr = 8.6 with tg δ = 5.5·10-5 for marble, and εr = 10-j3 for asphalt. For marble, the complex part of permittivity can be neglected for reflection estimation purposes. For vertical polarization the reflection coefficient can be determined using the following formula [14]:

$$\rho_V = \frac{\varepsilon_r \cdot \sin\psi - \sqrt{\varepsilon_r - \cos^2\psi}}{\varepsilon_r \cdot \sin\psi + \sqrt{\varepsilon_r - \cos^2\psi}} \tag{6}$$

where ψ is the incidence angle (between secondary ray and floor plane). It can be observed that $\psi = \theta - \pi/2$.

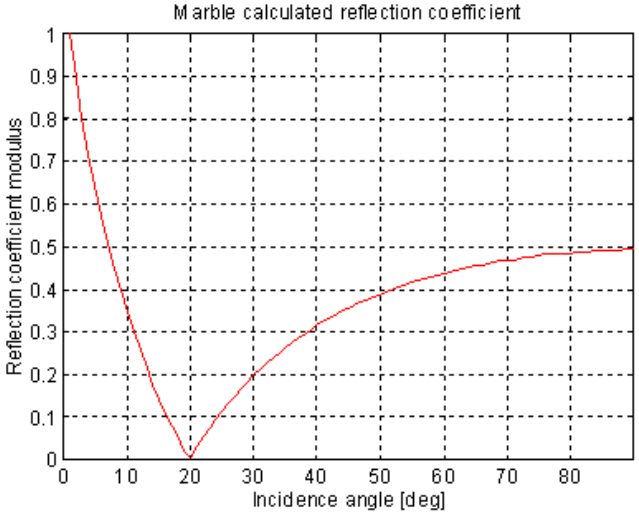

Figure 2. Modulus of reflection coefficient of the marble floor vs. incidence angle – equation (6)

It can be seen from Fig. 2 that the reflection coefficient cannot be totally neglected, since it can alter the signal with 3dB over 20 degrees incidence, and more for lower angles. Variation in our case is between 0 (at about 4.4 m from antenna, 20° incidence) and 0.43 (at 1m from antenna, 56° incidence). For long distances the received power can be written as [12]:

$$P_r = P_{eir} \cdot \left(\frac{\lambda}{4\pi \cdot r}\right)^2 \cdot \left|1 + \rho_v \cdot e^{j \cdot \Delta\varphi}\right|^2 \tag{7}$$

where $\Delta\varphi$ is the phase difference between rays (φ here is not the azimuth).

Since we are considering short distances, and taking into account all the attenuations, the received power is in our particular case can be determined using the following formula:

$$P_r = P_{eir} \cdot \left(\frac{\lambda}{4\pi \cdot r}\right)^2 \cdot \left|1 + \rho_v(\psi) \cdot \sqrt{G_d} \cdot \cos^{p+1.37+1}(\psi) \cdot \exp\left(j \cdot \frac{2\pi}{\lambda} r \cdot \frac{1-\cos\psi}{\cos\psi}\right)\right|^2 \tag{8}$$

where: $\psi = arctg(h/r)$ and G_d is receiving antenna gain (the dipole). Dipole pattern ($HPBW_{ver}$ = 78°) is simulated with [22]:

$$G_{dip}(\theta, \varphi) = G_d \cdot \sin^{2\times 1.37}\theta \tag{9}$$

and θ replaced with ψ, therefore the *sin* function is replaced with *cos* – see explanation after (6).

Also, the cos exponent *p+1.37+1* comes from three parts: *p=2.41* is the same from (2) and (4), *1.37* comes from dipole (9) and *1* is due to the ratio of the distances: direct versus total reflected ray length are in ratio of cos ψ as the attenuation difference between the direct and reflected optical paths is not neglectable for short distances. The term $r \cdot \frac{1-\cos\psi}{\cos\psi}$ is the length difference between the direct and reflected rays and represents the phase difference. Formula (8) takes into account only the ground reflection, the strongest in our setup. For a complete analytic model it would have been necessary to take into account another four weaker reflections: one from the ceiling, one from front wall and also two from lateral walls (which are to be taken into account with horizontal reflection coefficient, whose formula is similar, but not identical with the vertical one). Models used in this paper are in fact a simple, one ray model (5) and a two ray model (8).

We have performed Matlab simulations according to the previously described method in order to determine the amount of expected power which can be obtained at the input of the receiving antenna using both the 1 ray and 2 ray propagation models and considering marble and asphalt ground reflections. The results are presented Section V where they are compared with those obtained through in field analysis of the energy harvesting system.

IV. Measuring Harvested Power

In order to determine the harvesting capabilities of the previously described system and compare them to the ones obtained through modelling, a setup for measuring has been devised which we will further describe.

For determining the output current, a closed loop Hall sensor system consisting of two current transducers one used for measuring and the other as reference has been used, ensuring minimal interference with the harvesting circuit [23]. For the measurement of the output voltage over different loads, a National Instruments USB 6251 data acquisition system (DAQ) [24] has been used.

To be able to interpret the value of the actual current that flows through the transducer and compensate for the fabrication differences between the two transducers, an automated calibration program was implemented in National Instruments LabVIEW 2009 development environment. A 10 kΩ resistor was connected to the cooper wire of the upper transducer. We have created a virtual instrument (VI) that controls an Agilent N6700B profile modular power system mainframe DC power source equipped with a 35V N6744B DC Power Module. The VI prescribes a voltage ranging from 0 to 32V DC with a step of 100 mV resulting in a measured current from 0 to 3.2 mA with a step of 10μA. The output voltage of the current measurement system and the prescribed currents were stored in the form of a compensation table together with the slope between two consecutive points. These measurements have later been used for self-calibration of the automated measuring system when performing in field measurements. The block diagram representation of the measuring setup can be seen in Fig. 3.

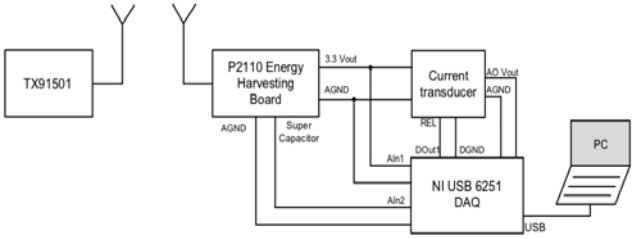

Figure 3. Measurement setup block diagram

As can be seen from Fig. 3, the boosted 3.3 output of the P2110 energy harvester board is connected to an analog input of the NI DAQ board. Also, at the output of the board, a resistive load of 5 kΩ can be connected by controlling the relay on the Hall sensor system board, and the prescribed current is read also by connecting the output of the current

measurement system to an analog input of the DAQ.

The energy harvested by the RF-DC converter on the P2110 integrated circuit is stored in a super capacitor which in turn powers the boost converter when the voltage reaches 1.8 V. The voltage drop over the super capacitor is also measured using the DAQ system.

The control of the DAQ is performed with a NI VI that we have developed which measures all previously mentioned voltage drops and stores them in files together with the time the samples have been acquired. The VI also performs internal filtering on the signals using a 2nd order Butterworth filter with a cutoff frequency of 1Hz.

At startup, the VI performs auto-calibration of the current measurement system by acquiring its output voltage and setting the 0 level, for a period of 60 seconds. The actual output voltage level of the amplifier is converted into current using the reference compensation table previously generated during calibration and also using interpolation between points.

V. Experimental Results

The evaluation of the system using the previously described measurement setup has been performed in two different environments, a hallway (Fig. 4a) and a parking lot (Fig. 4b).

a.

b.

Figure 4a. Hallway measurement setup 4b. Parking lot easurement setup

Both transmitter and receiver have been placed at the same height of 1.5m. Measurements have been acquired by placing the transmitter at different distances from the P2110 energy harvesting board beginning from 2m until the circuit was no longer able to harvest any energy. This behavior was noticed at a distance between transmitter and receiver of 8 meters for the hallway and 14 meters for the parking lot.

We have processed the measurements and calculated the average output power of the energy harvesting board over a 5 kΩ load resistor. We have chosen a resistive load of this size because the amount of energy available at the output of the harvesting board should be enough to power a microcontroller board equipped with sensors for data acquisition and a 2.4 GHz wireless transmitter. The results can be seen in Fig. 5.

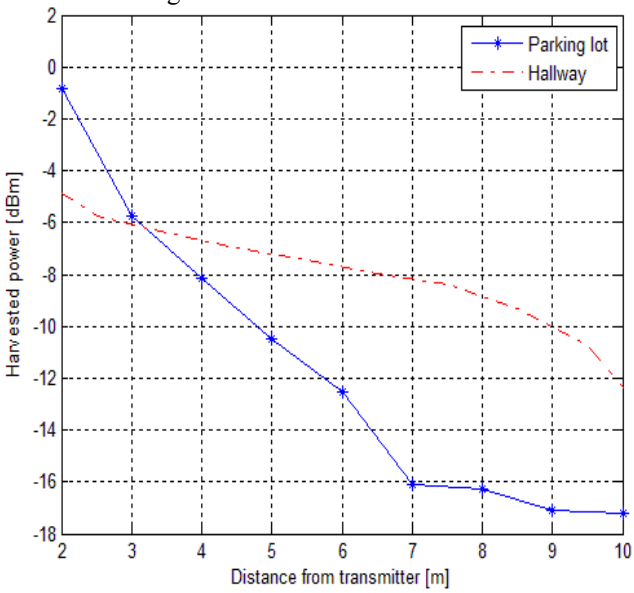

Figure 5. In line measurement – average harvested power vs. distance

As expected the average output power decreases with distance between the transmitter and receiver. However it can be seen that there is an up to 8 dBm difference between the amounts of energy the system can harvest in the two different environments. The effects of reflection and absorption from walls, ceiling and floor in the hallway has an impact on the amount of energy harvested which does not vary as abruptly as expected. After 10 meters however we have been unable to harvest any power in the hallway. On the other hand, the experiments performed in open space show a behavior closer to our expectations due to the fact that the environment has little effect on the receiving signal strength and only ground reflections intervene. In an open environment we have been able to harvest power with the P2110 circuit from distances up to 14 meters.

We have also analyzed the amount of harvested power of the system in an enclosed environment (a room) using two different experimental setups as can be seen in Fig. 6a and 6b.

In both situations the transmitter was placed in a fixed position on a wall at a height of 1.5 meters from the ground and the receiver was also placed at the same height during all measurements.

a.

b.

Figure 6a. Harvested power analysis setup 6b. Spectral analysis setup

In Fig. 6a the harvested power at the output of the P2110 energy harvester was analyzed using the experimental setup described in Section IV. The setup was placed on a mobile table and the tiles on the floor were used as distance markers. Measurements were performed by moving the table in a matrix at each intersection of the tile beginning from 1 meter away from the transmitter. The step used was of 42.5 cm, the diagonal of the tile. As a result we have obtained a map with the available power at each point in the matrix. The maximum front distance we have measured was of 4.85 m and the maximum lateral distance was of 3.4 m.

Under the same conditions we have also performed measurements using the Agilent N9320B RF Spectrum Analyzer as can be seen in Fig. 6b to determine the available energy at the input of the RF-DC converter.

The obtained results were used to create a power map which is depicted in Fig. 7. The map also contains the power levels resulted from modelling and simulation using the 1-ray and 2-ray ground reflection model.

It can be seen that in the case of indoor propagation there are little differences between the two simulation models. The 2-ray model resembles best with the original, but in terms of error, both are in the same range of 5dBm maximum error, mainly at large distances with 2.1dBm standard deviation.

a.

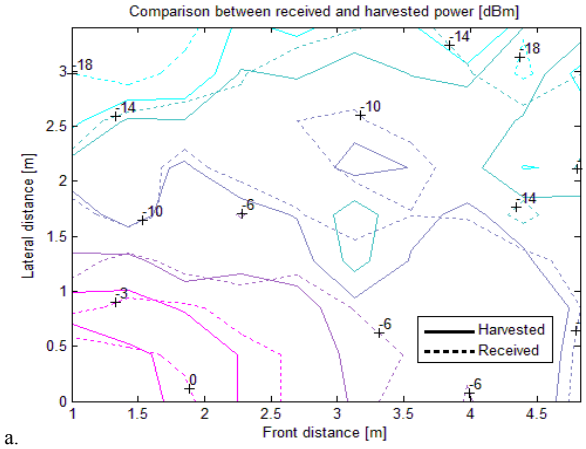

b.

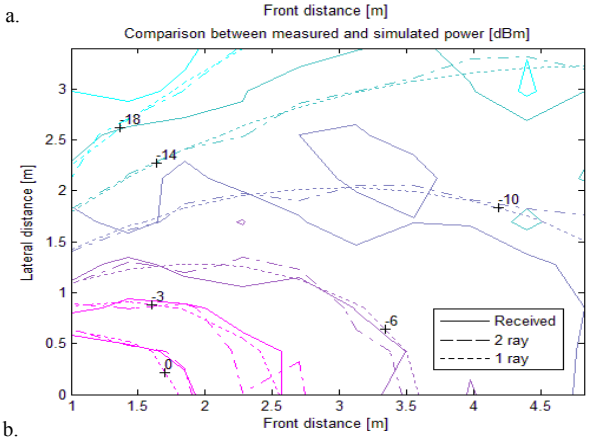

Figure 7a. Harvested vs. received power levels 7b. Received vs. 2 ray vs. 1 ray power levels

a.

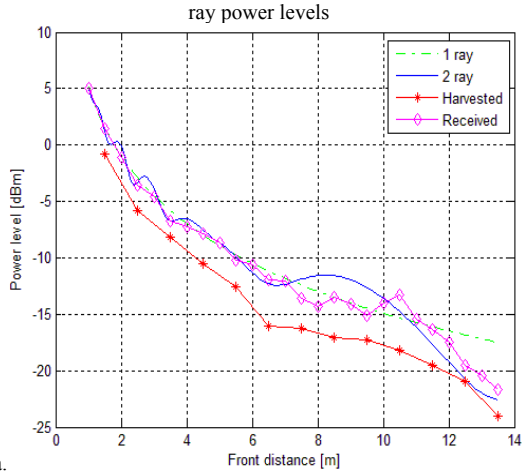

b.

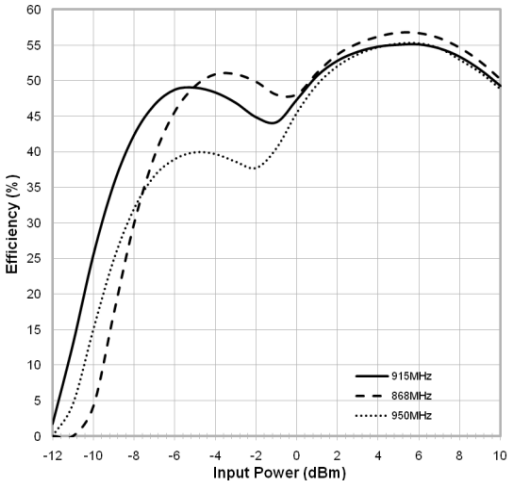

Figure 8a. Indoor harvested vs. received vs. modelled power, in line on maximum radiation direction 8b. Powerharvester efficiency vs. RF_{IN} (dBm) [9]

As can be seen from Fig. 8a there is a difference between received and harvested power. The efficiency of the power harvester can go as low as 1% or less for input levels below -12dBm [9] as can be seen from Fig. 8b. Since the manufacturer does not provide a detailed documentation about the input circuit, it is difficult to obtain an accurate prediction for the harvested power at low levels. As can be observed from Fig. 8a the harvested power is lower than the received power due to the efficiency of the RF-DC and Boost converters circuit. However we have noticed that the measured efficiency of the circuit exceeds the manufacturers' specifications and at -20 dBm input power the efficiency of the circuit is still over 20% and not below 1% as can be seen from Fig. 8b. This can be due to other unexpected RF fields existent in the measurement environment.

VI. Conclusions and Future Work

This paper describes the methodology used for analyzing the performance of the Powercast P2110 915MHz RF energy harvester. We have performed in field experiments using a measurement system that we have developed which is made up of a current measuring system and a NI DAQ. We have also developed the programs that perform calibration and measurement of output power. We have modelled the power characteristics of the system through simulations using the Matlab environment based on formulas existent in literature. For a more accurate model we have considered ground reflections and we have calculated the reflection coefficients of the two different surfaces on which we have performed measurements on.

Comparing in field results with the ones obtained through modelling, using the one ray and two ray models and beam-shaped antenna patterns in the 5 meters range of the radiation beam, we have managed to predict the received power level within 2dBm dispersion. As can be observed, the two ray model resembles best with the measured received power map, but does not increase the precision of modelling despite its second ray complicated formula.

There are some differences in terms of harvested power between the two environments (indoor and outdoor) which come from variations of the received signal level due to environmental reflections, but also from different efficiency. We have noticed that below -10dBm input power level prediction is very difficult. Since the datasheet operating limit is -11.5dBm input power one can conclude that the examined system has a 5 to 6 meters range in the main lobe of radiation.

As future research directions we plan to study the impact of using until five rays reflection model on enclosed environments to determine if we can improve the estimation of received power. We also plan to determine suitable applications for such systems using mainly the two ray model for power transfer which has been proved sufficiently accurate. Using the obtained results we plan to research optimum placement solutions for energy harvesting systems for maximum efficiency of the harvested power.

References

[1] M. Durisic, Z. Tafa, G. Dimic, V. Milutinovic , "A survey of military applications of wireless sensor networks", 2012 Mediterranean Conference on Embedded Computing, pp. 196-199, 2012

[2] D. Puccinelli, M. Haenngi, "Wireless sensor networks: Applications and challenges of ubiquitous sensing", IEEE Circuits and Systems Magazine, Vol. 5, Issue 3, pp. 19-31, 2005

[3] M. Barnes, C. Conway, J. Mathews, D. Avrind, "ENS: An energy harvesting wireless sensor network platform", 5th International Conference on Systems and Network Communications (ICSNC'10), pp. 83-87, 2010

[4] S. Roundy, D. Steingart, L. Frechette, P.K. Wright, and J.M. Rabaey, "Power Sources for Wireless Sensor Networks", In Proc. EWSN, 2004, pp.1-17.

[5] S. L. Kumar, M. E. Posner, P. Sinha, "Optimal sleep-wake up algorithms for barriers of wireless sensors," Fourth International Conference on Broadband Communications, Networks and Systems (BROADNETS '07), pp. 327 – 336, Sept 2007.

[6] W. B. Heinzelman, A. P. Chandrakasan, H. Balakrishnan, "An application-specific protocol architecture for wireless microsensor networks," IEEE Transactions on Wireless Communications, Vol. 1, Issue 4, pp. 660-670, 2002.

[7] I.F. Akyildiz, W. Su, Y. Sankarasubramaniam, E. Cayirci, "A survey on sensor networks," in IEEE Communications Magazine, pp. 102–114, Aug. 2002.

[8] T. Le, K. Mayaram, T. Fiez, "Efficient Far-Field Radio Frequency Energy Harvesting for Passively Powered Sensor Networks," IEEE Journal of Solid-State Circuits, Vol. 43, Issue 5, 2008, pp. 1287-1302.

[9] Powercast P2110 – 915 MHz RF Powerharvester Receiver, Product Datasheet Rev A, 2010, http://www.powercastco.com/PDF/P2110-datasheet.pdf, Last visited on 19.09.2012.

[10] Powercast P2110-EVAL-01 Energy Harvesting Kit for Wireless Sensors, User's Manual, 2010, http://www.powercastco.com/PDF/P2110-EVAL-01-manual.pdf, Last visited on 19.09.2012.

[11] Powercast TX91501 – 915 MHz Transmitter User's Manual. 2010 Rev A, http://www.powercastco.com/PDF/TX91501-manual.pdf, Last visited on 19.09.2012.

[12] A. Ignea, E. Marza, A. De Sabata, "Antene si Propagare" (English title: "Antennas and Propagation"), Editura de Vest, ISBN 973-36-0351-1, pp. 82, 2002.

[13] C. A. Balanis, "Modern Antenna Handbook," John Wiley & Sons, Inc, ISBN-10: 0470036346, pp. 3-56, 2008.

[14] A. Ignea, "Compatibilitate Electromagnetica" (English title: "Electromagnetic Compatibility"), Editura de Vest, ISBN 978-973-36-0453-2, 2007, pp. 55.

[15] ISO 31-11:1992 Quantities and units -- Part 11: Mathematical signs and symbols for use in the physical sciences and technology

[16] T. Petriţa, "Approximation of antenna diagram for BTS antennas," in Proc. TSP2011, pp. 257 – 260, Budapest, Hungary, 2011.

[17] W.L. Stutzmann, "Estimating Directivity and Gain of Antennas", IEEE Antennas and Propagation Magazine, Vol. 40, No.4, 1998

[18] T.G. Vasiliadis, A.G. Dimitriou, G.D. Sergiadis, "A Novel Technique for the Approximation of 3-D Antenna Radiation Patterns", IEEE Transactions on Antennas and Propagation, Vol. 53. No.7. July 2005

[19] R.P. Singh, M.P. Lal, T. "Laboratory measurement of dielectric constant and loss tangent of Indian rock samples", Annals of Geophysycs, Vol.33, No.1,1980

[20] Zhang, B., Zhong, Y., Liu, H.,Wang, F.,"Experimental Research on Dielectric Constant Model for Asphalt Concrete Material, Advanced Materials Research, Vols.250-253, 2011

[21] J. Baker-Jarvis, M. D. Janezic, R. F. Riddle, R. T. Johnk, P. Kabos, C. Holloway, R.G. Geyer, C.A. Grosvenor, "Measuring the Permittivity and Permeability of Lossy Materials: Solids, Liquids, Metals, Building Materials, and Negative-Index Materials," NSIT technical note, 2005, pp.142

[22] T. Petrita, Comparison of two approximation models for near-field of BTS antennas, in proc. TSP2012, Prague, Czech Republic, 2012

[23] C. Cirstea, M. Cernaianu, A. Gontean., "An Inductive System for Measuring Microampere Currents", IEEE 18th International Symposium for Design and Technology in Electronic Packaging (SIITME 2012), 2012, pp.197-200

[24] National Instruments 6251 multifunction data acquisition system http://sine.ni.com/nips/cds/view/p/lang/ro/nid/202802, Last visited on 19.09.2012.

[25] Agilent N9320B RF Spectrum Analyzer 9kHz to 3 GHz, http://cp.literature.agilent.com/litweb/pdf/5990-8119EN.pdf, Last visited on 19.09.2012.